 doi:10.20944/preprints202205.0371.v1

Article

Removal of Diclofenac-Na from Aqueous Solution onto H_3PO_4 Modified Composite Clay

Ajani, Ayobami Olu[1,2], Adeniji, Ademola Toheeb[1,2,4], Ayodabo, Shina Samson[1,2], Alade, Abass Olanrewaju [1,2,3*], Afolabi, Tinuade Jolaade [1,2] and Ganiyu, Ololade Sofiat[1, 2]

[1] Department of Chemical Engin7eering, Ladoke Akintola University of Technology, Ogbomoso, Nigeria
[2] Bioenvironmental, Water and Engineering Research Group (BWERG), Ladoke Akintola University of Technology, Ogbomoso, Nigeria
[3] Science and Engineering Research Group (SAERG), Ladoke Akintola University of Technology Ogbomoso, Nigeria
[4] Department of Chemistry, Universidade do Porto, Porto, Portugal
*Corresponding author: aoalade@lautech.edu.ng; +2347037885961

Abstract: Under batch experiment conditions, this work seeks to successfully remove Diclofenac-Na (DCF-Na) from an aqueous solution utilizing a composite sorbent made of Bentonite, Kaolinite clay, and Worm casting (BKW). This study investigated the structural modification of the H_3PO_4 Modified Clay by X-ray fluorescence and the effect of selected adsorption factors – DCF-Na concentration and modified BKW composite dosage. The concentration equilibrium data was used to study six isotherm models. Freundlich isotherm model better explained the adsorption of DCF-Na onto modified BKW composite with a correlation coefficient close to 1. Kinetics models were examined, and the Elovich model gave a better fit than other kinetic models studied. Mass diffusion mechanisms and thermodynamics studies were successfully carried out. The enthalpy change values evaluated were negative, which revealed the spontaneity of DCF-Na remediation onto modified BKW, and that DCF-Na adsorption is exothermic and occurred through a physisorption process.

Keywords: Bentonite-Kaolinite-Worm Cast Clay; composite; Diclofenac-Na; geosorption; wastewater

1. Introduction

Diclofenac-Na (DCF-Na) is an analgesic and anti-inflammatory drug often used to relieve pain during diseased condition. DCF-Na can be administered orally or applied to the skin [1]. Zhang et al., in 2008, estimated the global consumption of DCF on annual basis to be 940 Tonnes from the International Marketing Services (IMS) health data. In 2011, DCF sales were anticipated to be $1.61 billion, representing an annual growth rate of 15.5 % [2]. According to recent reports, traditional and developed markets such as the United States, China, India, and Brazil consume approximately 60 Tonnes of DCF-Na per year [3]. Furthermore, DCF-Na is included in the Emergency Medical List of 74 countries. DCF-Na intake is thought to be on the rise in North America in recent years, as ailments including arthritis and heart disease have become more frequent [2] .

Due to the lack of veterinary consumption statistics, estimating total DCF-Na consumption is now rather difficult. DCF-Na has recently been discovered to be harmful to human health and terrestrial organisms. In India, the manufacture and use of DCF-Na for veterinary purposes was outlawed in 2006 [4]. Diclofenac-Na (DCF-Na) in aqueous solutions, even at trace amounts, has been shown in toxicological investigations to have negative effects on human life, flora, and animals [5]. Despite the fact that pharmaceutical medications are designed to treat human allergies, they may have negative consequences for the environment. When these medications enter the atmosphere, they may have a similar effect in animals with similar target cells, organs, tissues, and systems [6].

Preprints (www.preprints.org) | NOT PEER-REVIEWED | Posted: 27 May 2022 doi:10.20944/preprints202205.0371.v1

Recently, there has been a persistent revelation of pharmaceutical drugs in industrial and spent waters [7]. Several treatment methods such as irradiation technology, photocatalytic degradation process, ozonation, Ion exchange have been used to treat DCF-Na, yet, the methods exhibit certain drawbacks such as high operational and capital cost. The adsorption process shows high efficiency to remediate these kinds of pollutants [8]. To this effect, economical and innovative adsorbents such as Kaolin, Bentonite, Zeolite, Worm cast, and Smectite, which are readily accessible, are presently being used to remove pharmaceuticals from their aqueous mixture.

Clay is widely used for pharmaceutical remediation due to its widespread availability, low cost, large surface area, excellent mechanical and chemical resilience, and a variety of structural and surface qualities. The adsorption capacity of clay is determined by its pore structure and chemical composition. Clays are quite simple to manipulate and effective for a variety of applications, including adsorption [6]. Under batch testing, this study aims to successfully remove Diclofenac-Na (DCF-Na) from wastewater using a composite sorbent made of Bentonite, Kaolinite clay, and Worm casting (BKW).

2. Methodology

2.1. Materials

Kaolinite and Bentonite Clay were sourced from Abakaliki deposits, Ebonyi State, Nigeria, and Worm Casting was obtained from LAUTECH in Ogbomoso, Nigeria, and then reduced to particle sizes ranging from 20 to 45 microns. The dry materials were crushed and sieved one more to a particle size of 75 microns. Each clay was treated in the same way. The study of surface modification was carried out using XRF (X-ray fluorescence) and SEM (Scanning Electron Microscopy. H_3PO_4 (Phosphoric Acid) and NaOH (Sodium Hydroxide) were provided by Bond Chemicals Industries Limited in Oyo, Nigeria. Diclofenac-Na was purchased from Akol Pharmaceutical, Ogbomoso, Oyo State, Nigeria.

2.2. Equipment

The equipment used includes Electric Oven (Saisho, S 936, Temperature 250°C, Time 60 mins), Rotary Shaker (HZ 300, Max 300 rpm, 960 mins), Digital Weighing balance (DT 502A, Max 500g, d = 0.01g), UV Spectrophotometer (UV-VIS Spectrophotometer, Model No U V752(D), Axiom Medical Ltd, UK), SEM (Scanning Electron Microscopy, JEOL, JSM 6500F), Crusher, pH meter, burette, Centrifuge, Laboratory Mortar, and Pestle.

2.3. Adsorbent Preparation

On collecting the clays (Bentonite, Kaolinite, and Worm casting), pebbles and undesired materials were sorted from the clays samples. The sieving process was subsequently carried out through a mesh (240 microns) to cast out large particle fractions of clay. The clays samples were dispersed (80 g) in distilled water (100 ml), heated, and filtered to remove suspended unwanted particles. The filtrates were allowed to settle and decanted after 24 hours. The resulting suspended clays were dried for 2 hours at 120 °C. The clays were ground and sieved to acquire particle sizes with a laboratory mortar and pestle [9]. The process was done individually for the clays. The samples were then ready for modification.

2.4. Acid Activation of the Clays sample

The prepared clay samples (80 g) were added into three different flasks (250 ml capacity) and were modified with concentrations (0.5, 1.5, and 2.5 mol/l) of Phosphoric acid. The suspension was heated for 2 hours on a magnetically stirred hot plate at 90 °C with 150 rpm agitation. At the end of the experiment, the resultant slurry was put through a Buchner funnel to separate the acid from the clay. The remaining clay was rinsed multiple times with distilled water to remove phosphate ions and other inorganic matter that may be present until a pH indicator indicated a neutral pH . The clay residues were dried for 2 hours at 120 °C in an oven [9]. The dry materials were crushed and sieved one more to

Preprints (www.preprints.org) | NOT PEER-REVIEWED | Posted: 27 May 2022 doi:10.20944/preprints202205.0371.v1

a particle size of 75 microns. Each clay we treated in the same way. To study the effect of the clay surface modification, the clay samples were investigated using XRF (X-ray fluorescence) and SEM (Scanning Electron Microscopy).

2.5. Preparation of DCF-Na

DCF-Na solutions for adsorption experiments were prepared from a stock solution (1 g) of DCF-Na (500 mg/l pH: 7.0) in 1000 ml of water [10]. The solution was stirred continuously to obtain a homogeneous solution. The solution was allowed to cool and then diluted to mark in a 1000 ml volumetric flask. The different concentrations needed for the research work were taken from the 1000 mg/l solution by serial dilution.

2.6. Adsorption Study of DCF-Na

The modified BKW composite adsorption performance was evaluated by carrying out an adsorption study using a traditional batch equilibrium technique [11]. The adsorbents (H_3PO_4 modified BKW composite) adsorption rates were evaluated from the sorption of DCF-Na before and after adsorption until equilibrium was reached. At room temperature and a known agitation rate in revolutions per minute, 1 g of acid-modified BKW composite was added to 100 ml of 200 mg/l concentrations of DCF-Na solutions for the sorption process [12]. The centrifuge was used to separate the content, and it was examined employing UV-Spectrophotometer at its wavelength of 300 nm[13]. The adsorption capacity was evaluated using equation 1, and the removal percentage was determined by equation 2:

$$\text{Adsorption capacity}\left(\frac{\text{mg}}{\text{g}}\right) = \frac{(\text{C}_{0-}\,\text{C}_\text{e}) \times \text{V}}{\text{M}} \quad (1)$$

$$\text{Removal}(\%) = \frac{\text{C}_0 - \text{C}_\text{e}}{\text{C}_0} \times 100 \quad (2)$$

Where C_o and C_e (mg/l) are the initial concentration and the equilibrium concentration of DCF-Na, M is the adsorbent mass in grams and V is DCF-Na volume in litres.

2.7. Adsorption Isotherm Models

Adsorption isotherm took place at room temperature using the batch mode process using 1 g of Modified BKW clay composite at five (5) DCF-Na solution initial concentrations (5, 10, 15, 20, and 25 mg/l) with neutrality maintained. The solution was vigorously shaking to reach equilibrium between 15–155 mins. The agitation speed (150 rpm) was constant for each run to ensure equal mixing. The content was centrifuged at 300 rpm for 10 min, and the supernatant solution in each flask was analyzed using UV-Vis Spectrophotometer for residue DCF-Na content. Six (6) isotherm models (Table 1) were used in this study which include Langmuir, Freundlich, Temkin, Harkin-Jura, Dubinin-Radushkevich, and Redlich-Peterson Isotherm models. The constants of these models were assessed after they were fitted to the adsorption equilibrium data.

2.8. Adsorption Kinetics Models

The kinetic studies helped determine the adsorption control mechanism onto activated Carbon and the rate-limiting step. Pseudo-first order, Pseudo-second order, Elovich, and Avrami models were the kinetic models (Table 1) that were employed to evaluate the experimental data.

Preprints (www.preprints.org) | NOT PEER-REVIEWED | Posted: 27 May 2022 doi:10.20944/preprints202205.0371.v1

Table 1. Non-Linear and Linear form of the Isotherm, Kinetic, and Diffusion models adopted for the removal of DCF-Na onto modified BKW composite.

Isotherm Model	Non-Linear form	Linear form	Linear plot	References
Langmuir	$q_e = \frac{(q_m K_L C_e)}{1 + K_L C_e}$	$\frac{C_e}{q_e} = \frac{1}{q_m K_L} + \frac{C_e}{q_m}$	$\frac{C_e}{q_e}$ vs. C_e	[15]
Freundlich	$q_e = K_F C_e^{1/n}$	$logq_e = logK_F + \frac{1}{n} logC_e$	$logq_e$ vs. $logC_e$	[15]
Harkin-Jura	$q_e = \left(\frac{A_H}{B_2 - logC_e}\right)^{\frac{1}{2}}$	$\frac{1}{qe^2} = \frac{B}{A} - \frac{1}{A} logC_e$	$\frac{1}{qe^2}$ vs. $logC_e$	[16]
Temkin	$q_e = Ln(AC_e)^B$	$q_e = BlnA + BlnC_e$	q_e vs. lnC_e	[15]
Dubinin-Radushkevich	$q_m = q_{ee^{\beta\epsilon^2}}$	$\ln q_e = \ln q_m - \beta E^2$	$\ln q_e$ vs. E^2	[15]
Redlich-Peterson	$q_e = \frac{AC_e}{1 + BC_e^{\beta}}$	$ln\frac{C_e}{q_e} = \beta lnC_e - \ln A$	$ln\frac{C_e}{q_e}$ vs. lnC_e	[17]
Kinetics Model				
Pseudo First Order	$q_t = q_e(1 - e^{-K_1 t})$	$\ln(q_e - q_t) = lnq_e - K_1 t$	$ln(q_e - q_e)$ vs. t	[15]
Pseudo Second Order	$q_t = q_e - \frac{q_t}{tK_2 q_e}$	$\frac{t}{q_t} = \frac{1}{K_2 q_e^2} + t/q_e$	t/q_t vs. t	[15]
Elovich	$q = \frac{1}{\beta} ln(1 + \alpha\beta t)$	$q = \frac{1}{\beta} ln(\alpha\beta) + \frac{1}{\beta} \ln t$	q vs. ln t	[16, 18]
Avrami	$q = q_e - q_e \exp(-kt^n)$	$ln\left(ln\frac{q_e}{q_e - q}\right) = nln\, k + nln\, t$	$ln\left(ln\frac{q_e}{q_e - q}\right)$ vs. $ln\, t.$	[18]
Diffusion Model				
Crank Diffusion (Boyd) Model	$\frac{\partial q}{\partial t} = \frac{D}{r^2}\frac{\partial}{\partial r}\left(r^2 \frac{\partial q}{\partial r}\right)$	$\frac{\bar{q}}{q_e} = 6\sqrt{\frac{Dt}{\pi R^2}}$	$\frac{\bar{q}}{q_e}$ vs. $\sqrt{t}.$	[19]
Vermeulen	$\frac{\bar{q}}{q_e} = \sqrt{1 - exp\left(-\frac{D\pi^2}{R^2}\right)}$	$ln\left(1 - \left(\frac{\bar{q}}{q_e}\right)^2\right) = -\frac{D\pi^2}{R^2}$	$ln\left(1 - \left(\frac{\bar{q}}{q_e}\right)^2\right)$ vs. t	[20]
Weber-Morris	Not Applicable	$q = k_{id}\sqrt{t} + B$	q vs. $\sqrt{t}$	[21]
Banghams	Not Applicable	$\log\left(log\frac{C_o}{C_o - q.m}\right) = log\left(\frac{k_0 m}{2.303}\right) + \alpha logt$	$\log\left(log\frac{C_o}{C_o - q.m}\right)$ vs. $logt$	[22]

2.9. Error Analysis

The adsorption isotherm and the kinetics models were validated using two different statistical error functions - Sum of Square Errors (SSE) and the Root Mean Square Error (RMSE) - in addition to Correlation Coefficient, R^2. The efficiency of the predictive model depends on lower error value. Microsoft Excel's Solver tool was deployed to estimate the adsorption isotherm parameters [14]. The error functions are given, as follows:

$$SSE = \sum_{i=1}^{N} \left(Q_{e,cal} - Q_{e,exp}\right)^2 \quad (3)$$

$$\text{RMSE} = \sqrt{\frac{1}{N}\sum_{i=1}^{N}\left(Q_{e,cal} - Q_{e,exp}\right)_i^2} \quad (4)$$

Where $Q_{e,cal}$ and $Q_{e,exp}$ are the adsorption isotherm calculated and experimental adsorbed amount, respectively. N represents the equilibrium data number.

2.10. Adsorption Diffusion Mechanism

Adsorption processes could either be physically or chemically controlled. This could either be by liquid film discussion, which involves the mass transfer rate process, or intra-

Preprints (www.preprints.org) | NOT PEER-REVIEWED | Posted: 27 May 2022 doi:10.20944/preprints202205.0371.v1

particle diffusion. This was achieved by varying concentrations, dosages, and temperatures against time for each mechanism studied.

2.11. Thermodynamics Studies

Thermodynamic studies investigate whether a reaction is spontaneous or not in an adsorption process. The Gibbs free energy change, ΔG°, indicates whether a reaction is spontaneous or not. Beakers (Eight) were charged into the thermostat incubator with shakers at varying temperatures of 40 ºC, 50 ºC, and 60 ºC. The concentrations in the beakers were kept constant at 10 mg/l, and the time was varied from 15 to 155 minutes at constant dosages of 1 g of modified BKW composite. The following equation gives the adsorption free energy when the adsorption equilibrium constant K_a is considered.

$$-RT \ln K_a = \Delta G^0 \quad (5)$$

Where ΔG° is the standard free energy change, J/mol, R is the universal gas constant, 8.314 J/mol K; and T is absolute temperature, K. Considering the relationship between ΔG° and K_a, change in equilibrium constant with temperature can be obtained in the differential form as follows:

$$\frac{dlnK_a}{dT} = \frac{\Delta H^0}{RT} \quad (6)$$

The Gibb's Free energy ΔG° is represented as follows:

$$\Delta G^0 = \Delta H^0 - T\Delta S \quad (7)$$

3. Results and Discussion

3.1. XRF Characterization

The X-ray fluorescence characterization revealed that the clay composition changed after modifications as presented in Table 2-4 for Bentonite, Kaolin, and Worm cast, respectively. The surface modification of the Clay samples improved their ion exchangeability by creating Bronsted Lowry acid sites and the exchange of interlayer catalytically positive ions and with other active positive ions. The presence of octahedral positive ions such as Mg^{2+}, Fe^{3+}, and Al^{3+} decreases considerably for the three clay samples, and that of tetrahedral positive ions such as Si^{4+} increased with acid modification. This is because, on acid modification, octahedral positive ions damage offers positive ions release to the solution, and the octahedral positive ion is suspended in the ion because of their insolubility [9]. In the presence of a high acid concentration, the resulting silica obtained polymerizes and deposits on yet to be destroyed silicate portions and shielding them from subsequent attack. The acid activation also causes a decrease in the exchangeable positive ions and an increase in the clay samples' surface area (Figure 1-3). The after effect is a result of impurities removal and exchange of replaceable positive ions (Na^+, Ca^{2+}, and K^+) with hydrogen ion (H^+), leaching of Al^{3+}, Mg^{2+}, and $Fe^{3+}$and clay de-lamination [9].

Preprints (www.preprints.org) | NOT PEER-REVIEWED | Posted: 27 May 2022 doi:10.20944/preprints202205.0371.v1

Table 2. XRF analysis of the modified and unmodified Bentonite clay.

Chemical Constituent (%)	NA	0.5 mol/l	1.5 mol/l	2.5 mol/l
Al_2O_3	27.9	20.4	13.9	5.7
SiO_2	46.6	59.8	72.5	89.2
Fe_2O_3	18.14	13.1	8.2	0.4
MgO	0.75	0.58	0.39	0.06
Na_2O	0.90	0.69	0.42	0.15
K_2O	0.49	0.42	0.28	0.09
CaO	0.06	0.06	0.04	0.01
TiO_2	2.16	1.87	1.21	0.75
LOI	3.03	2.76	1.76	0.92
Total	100	99.68	98.7	97.28
CEC (meq/100g)	58	51	44	28
Surface area (m^2/g)	28.6	35.7	40.3	63.8

NA: No Acid Modification

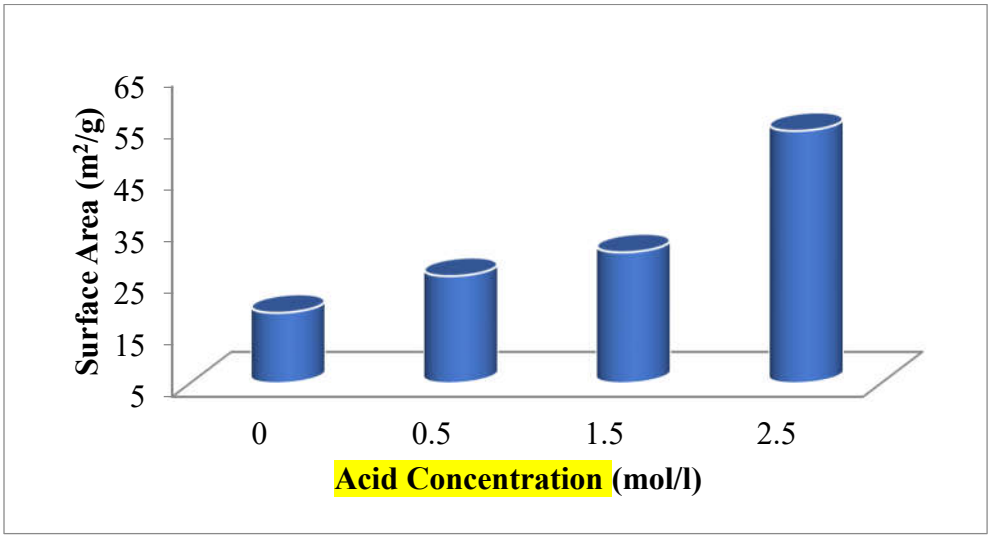

Figure 1. Variation of surface Area of the unmodified (UAM) and modified (0.5 , 1.5 , and 2.5 mol/l) Bentonite samples.

Table 3. XRF analysis of the modified and unmodified Kaolinite Clay.

Chemical Constituent (%)	NA	2 mol/l	4 mol/l	8 mol/l
Al_2O_3	26.9	21.45	17.04	13.97
SiO_2	48.6	57.8	63.93	68.64
Fe_2O_3	16.13	12.51	9.65	7.83
CaO	0.08	0.05	0.03	0.02
MgO	1.78	1.46	1.08	0.74
K_2O	0.11	0.07	0.05	0.03
TiO_2	2.06	1.74	1.36	1.01
LOI	3.67	2.73	2.25	1.92
Total	99.33	97.81	95.39	94.16
CEC (meg/100g)	97	78	63	57
Surface area (m2/g)	63	85	110	145

NA: No Acid Modification

Preprints (www.preprints.org) | NOT PEER-REVIEWED | Posted: 27 May 2022 doi:10.20944/preprints202205.0371.v1

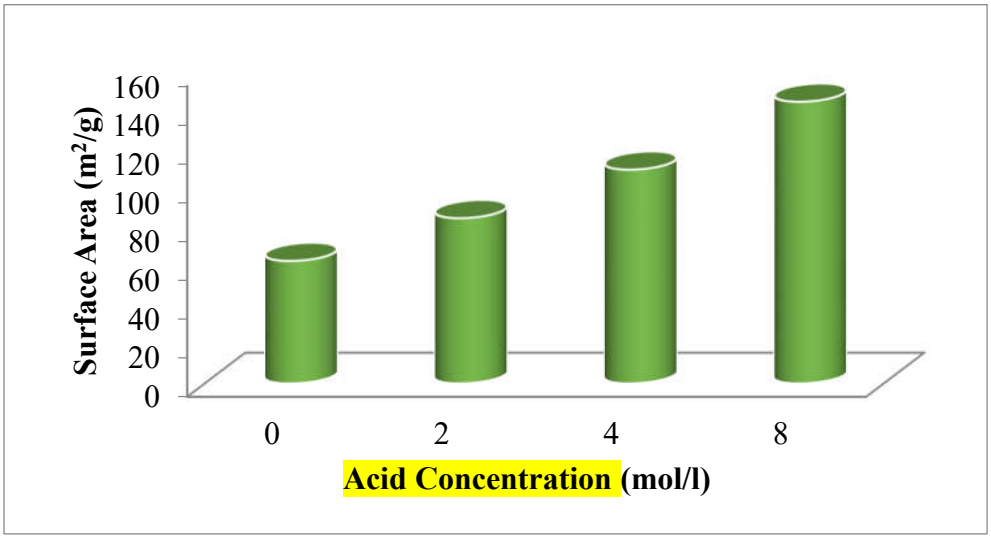

Figure 2. Variation of surface Area of the unmodified (UAM) and modified (2, 4, and 8 mol/l) Kaolin samples.

Table 4. XRF analysis of the modified and unmodified Worm cast Clay.

Chemical Constituent (%)	NA	2 mol/l	4 mol/l	8 mol/l
NaO	6.28	6.3	6.4	6.5
MnO	0.99	1	2	4
CaO	75.00	80	83	84
MgO	2.34	2.1	1.75	1.51
K_2O	1.23	1.26	1.29	1.4
Total	85.84	90.66	94.44	97.40
CEC (cmol/kg^{-1})	20.18	18.79	14.55	12.35
Surface area (m^2/g)	18.6	25.7	30.3	53.8

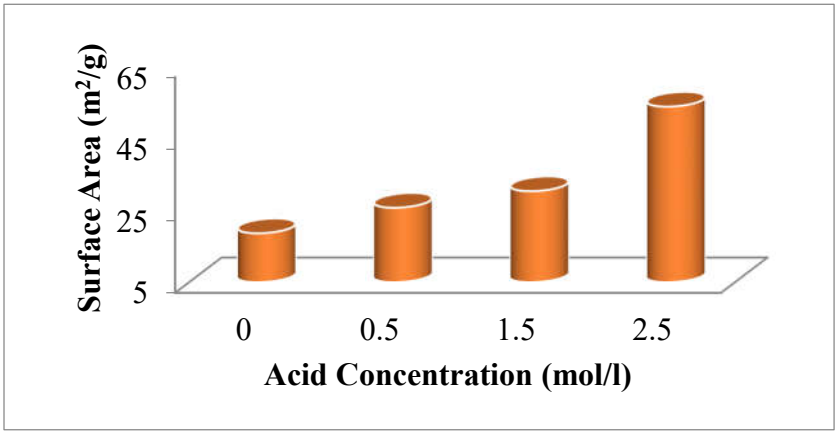

Figure 3. Variation of surface Area of the unmodified (UAM) and modified (2, 4, and 8 mol/l) Worm cast samples.

 doi:10.20944/preprints202205.0371.v1

3.2. SEM Characterization

Images of BKW clay components are shown in Figure 4. They depict the morphological examination of the raw and acid treated BKW components clay using scanning electron microscopy. The acid-treated bentonite and kaolin clays (figure 4, b and d) show an improvement in the surface area from the water-treated clays (figure4, a and c) with the presence of more heterogeneous layered sheets of various sizes. This is due to cations leaching from the clay surface, thereby creating more void - increase in porosity - on the clay surface [9]. Figures 4 e and f show the raw and acid-treated worm cast. The surface treatment of worm cast did not show any improvement in the surface morphology, which might be due to a very high concentration of acid used during activation [9].

3.3. Effect of Adsorption Factors on DCF-Na removal from modified BKW composites

The section discusses the results of the influence of selected adsorption parameters – concentration of DCF-Na and the amount of H_3PO_4 modified BKW composite – in DCF-Na adsorption process.

3.3.1. Effect of concentration of DCF-Na

The effect of concentration of DCF-Na in an aqueous solution on DCF-Na removal onto modified BKW composite was studied at 1 g of H_3PO_4 modified BKW composite of clay composition ratio of 1:2:1 for three different concentrations – 5, 10, and 15 mg/l. It was observed from the plot (Figures 5a, b) that the adsorption capacity (QE) and removal efficiency (RE) increased with increasing contact duration time from 15 to 155 minutes and increasing of concentration of DCF-Na. Also, the adsorption equilibrium was reached at 85 minutes for the three concentrations. The maximum adsorption capacities at 5 -15 mg/l are 0.343, 0.719 and 1.114 mg/g respectively corresponding to 68.5, 71.9 and 74.2% while the minimum adsorption capacities are 0.063, 0.256 and 0.508 mg/g respectively corresponding to 12.6, 25.6 and 33.9% removal efficiencies, respectively. The adsorption capacity and removal efficiency increase with the increase in concentration possibly because the adsorption sites as the adsorbent dosage increases as result agrees with results in similar studies conducted by [22-24] on the adsorption of DCF-Na on *Cyclamen persicum* tubers based activated Carbon, Natural and pillared clay, and activated carbon prepared from olive stones, Graphene Oxide, Amino-functionalized cellulose nanocrystals/chitosan composite, respectively.

Preprints (www.preprints.org) | NOT PEER-REVIEWED | Posted: 27 May 2022 doi:10.20944/preprints202205.0371.v1

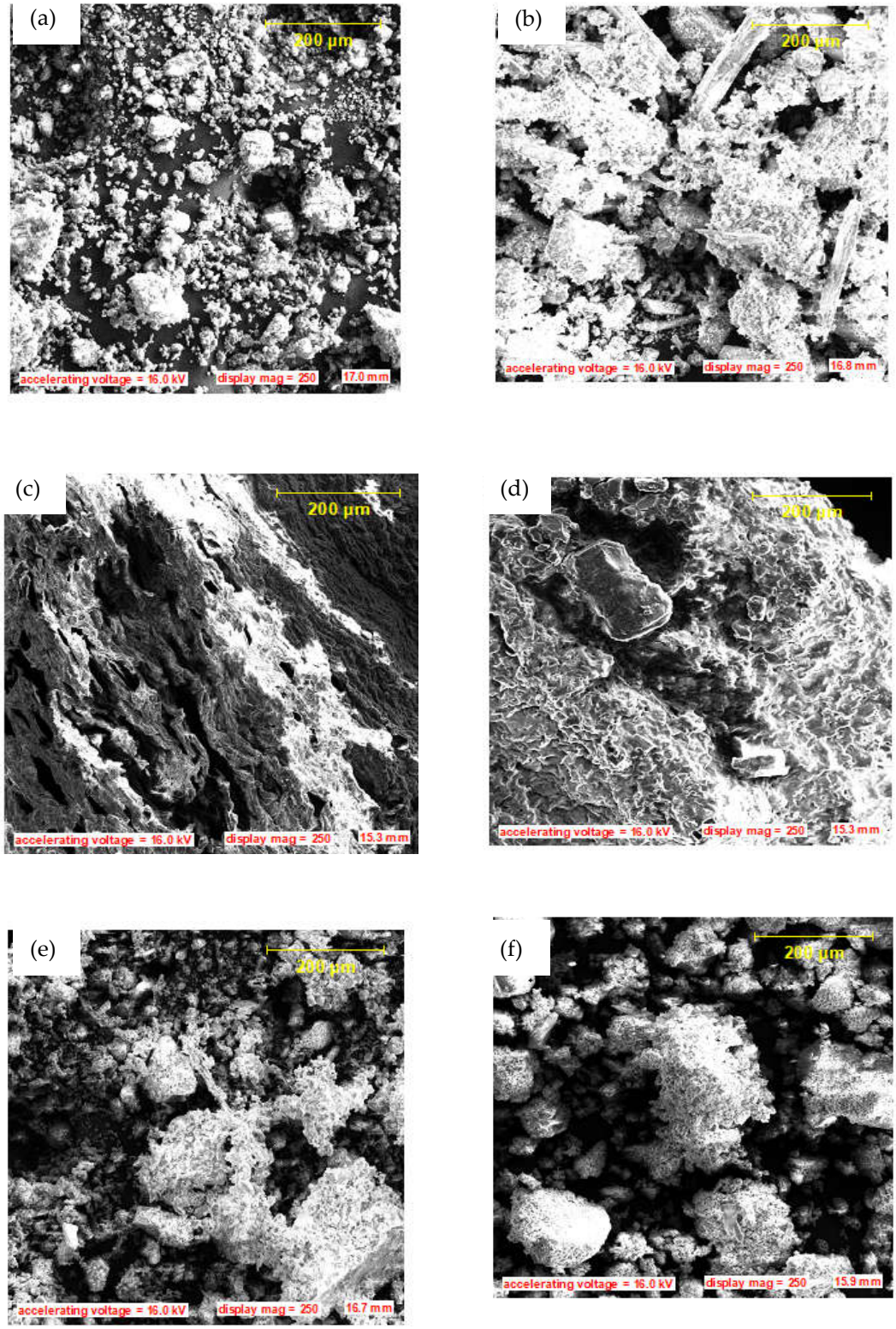

Figure 4. Scanning Electron Microscopy for modified and unmodified Bentonite (a and b), Kaolin (c and d), and Wormcast (e and f).

Preprints (www.preprints.org) | NOT PEER-REVIEWED | Posted: 27 May 2022 doi:10.20944/preprints202205.0371.v1

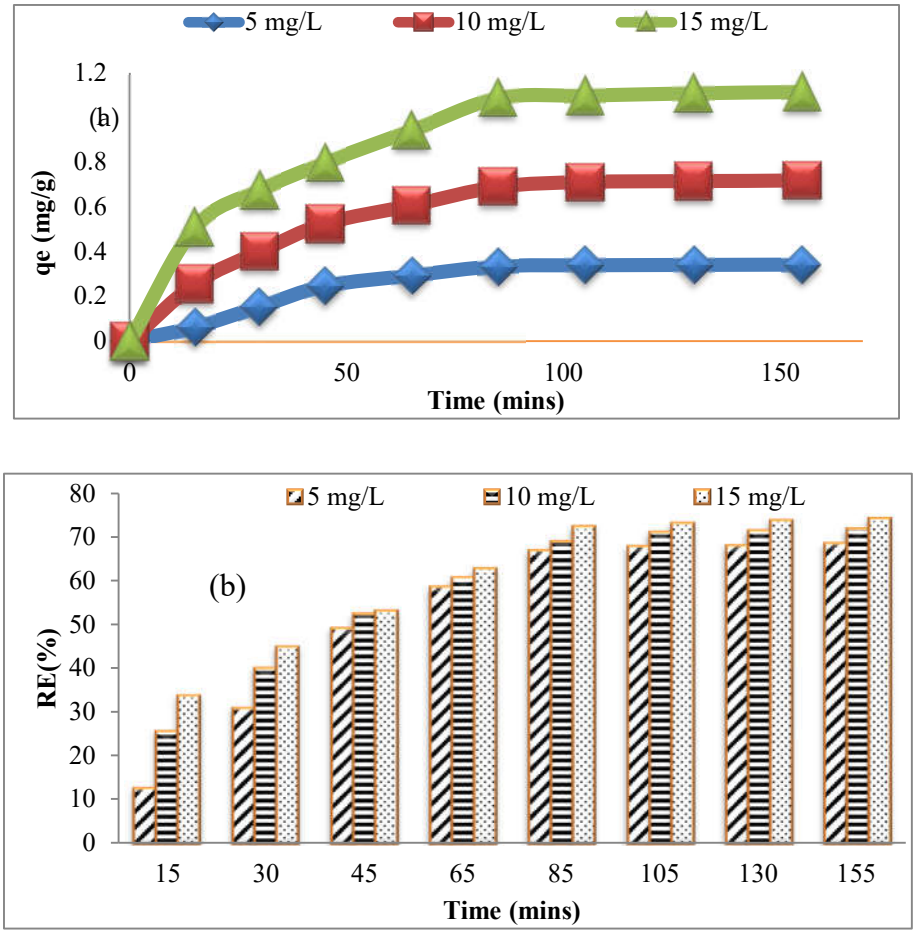

Figure 5. (a) Adsorption Capacity (b) Removal Efficiency (RE) plot describing the effect of concentration of DCF-Na using 1 g of H_3PO_4 modified BKW composite (1:2:1) at room temperature.

3.3.2. Effect of geosorbent dose on DCF-Na removal from solution onto modified BKW composite

At 10 mg/l of DCF-Na solution, the effect of geosorbent dose on DCF-Na removal from aqueous solution onto BKW composite was investigated for three different BKW composite doses (0.5, 1 and 1.5 g), as shown in Figure 6 a, b. The QE and RE increased with increasing duration from 15 to 155 mins. With increasing geosorbent dose, adsorption capacity dropped but overall removal efficiency improved. This is due to the presence of numerous available pores as the adsorbent increased and the total adsorbed DCF-Na were shared between these pores leading to a decrease in adsorption capacity per pore but there is an increase in the overall removal efficiency of the modified BKW adsorbent. Also, adsorption equilibrium was reached at 130 mins for the three dosages. The minimum adsorption capacities at 0.5, 1 and 1.5 g are 0.761, 0.472 and 0.375 mg/g, respectively, corresponding to 38.1%, 47.2% and 56.3% while the maximum adsorption capacities are 1.686, 0.840 and 0.567 mg/g, respectively, corresponding to 68.6, 84.0 and 90.1% removal efficiencies, respectively. The trend from the adsorption capacity results from the examined geosorbent demonstrates that as the geosorbent dose is increased, adsorption capacity drops while removal efficiency rises, which is consistent with reported results in the literature [22-25].

Preprints (www.preprints.org) | NOT PEER-REVIEWED | Posted: 27 May 2022 doi:10.20944/preprints202205.0371.v1

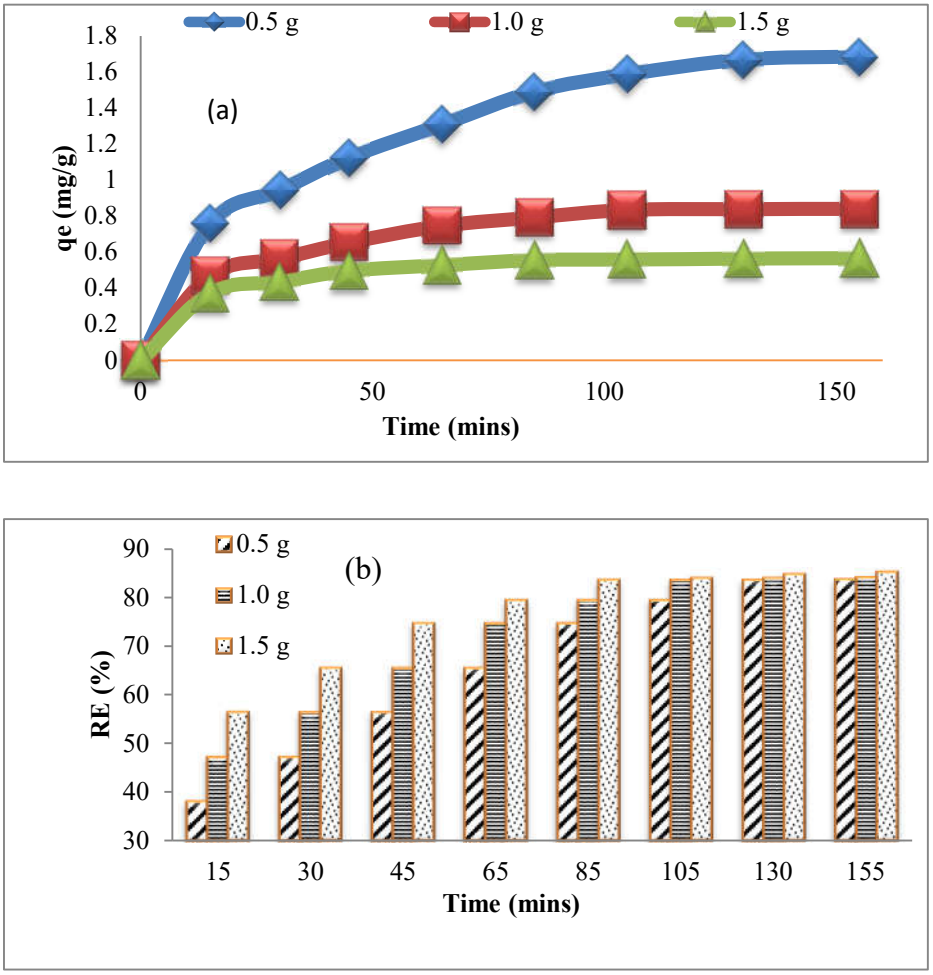

Figure 6. (a) Adsorption Capacity (b) Removal Efficiency (RE) plot describing the effect of geo-sorbent dose on the adsorption of 10 mg/l DCF-Na onto H_3PO_4 modified BKW composite (1:2:1) at room temperature.

3.4. Adsorption Isotherm Models

Figure 7 shows the six isotherm models - Langmuir, Freundlich, Harkin-Jura, Temkin, Dubinin-Radushkevich, and Redlich-Peterson, employed in fitting the experimental data of DCF-Na adsorption. Table 5 shows that the value of the models regression coefficients is more than 0.89 for all which examine the goodness of fit [23]. Given the fact that all binding sites have the same energy and are a finite number, the Langmuir model predicts monolayer adsorption. It also takes into account the fact that once the monolayer is formed, the maximum amount adsorbed may reach a limit [24]. The Langmuir constants are shown in Table 5. The Standard error, SSE and RMSE results of the Langmuir model were more than 2 order of magnitude higher than Freundlich isotherm model which shows that the model is unsuitable to describe the adsorbate sorption process.

Freundlich model (Figure 7b) is based on a heterogeneous adsorbent surface with changing energy levels at the adsorption sites [15]. When "n", the Freundlich constant, is between 0 and 1, a favorable adsorption process occurs and when "n" exceeds that range, it indicates that the adsorbent and the adsorbate have a greater connection. The value of "n" in Table 6 indicates that DCF-Na adsorption is favorable and a heterogeneous process with strong contact between the adsorbate and the adsorbent [25]. The value of "n" and the Freundlich constants are compared with similar studies (Table 7) on the adsorption of DCF-Na. The correlation coefficient, R^2, of 0.999 indicates that the Freundlich Isotherm model perfectly describes DCF-Na adsorption by BKW composite adsorbent [26]. Freundlich isotherm model gave the least Standard error, SSE and RMSE when compared to

 doi:10.20944/preprints202205.0371.v1

other adsorption models used in this study (Table 5). Thus, the adsorbate uptake onto the adsorbent sample can be described by the Freundlich isotherm model.

Harkin-Jura model accounts (Figure 7c) for the existence of multilayer and heterogeneous pore distribution [15, 30]. Table 5 summarizes relevant Harkin-Jura isotherm parameters. The correlation coefficient value of 0.9825 indicates that the BKW composite have an average fit for DCF-Na adsorption. The adsorption of DCF-Na on BKW composite obeys the multilayer adsorption rule, as shown by this finding. However, the error estimation results were on parity with the Langmuir isotherm, invalidating the model's prediction in explaining the DCF-Na adsorption process. However, the error estimation results were on parity with the Langmuir isotherm, invalidating the model's prediction in explaining the DCF-Na adsorption process.

The adsorbent-adsorbate interaction is represented by the Temkin isotherm model (Figure 7d). Temkin model assumes interactions between the adsorbent and the adsorbate without regard to low or high adsorbate concentrations [25]. At 25 °C, the Temkin parameter B, which is related to adsorption heat, was as high as 168 kJ/mol, implying a chemical adsorption process [27]. The Dubinin-Radushkevich isotherm model posits a multilayer structure with Van der Waal forces. It is a fundamental model that qualitatively depicts gases and vapors adsorption on microporous adsorbents [16]. The adsorption of DCF-Na to the tested BKW composite was consistent with the Dubinin-Radushkevich model (Table 5) [28]. Both the Temkin and Dubinin-Radushkevich model predictions are indeed valid and backed by the low error analysis result.

The Redlich–Peterson model combines Langmuir and Freundlich isotherms in a hybrid adsorption process. When the exponent, β, of the Redlich-Peterson equation is equal to 1, the Langmuir isotherm is preferred, and when it is equal to 0, Henry's rule takes over and behavior resembles that of the Freundlich isotherm [24]. The value of the Redlich–Peterson parameter 'β' (-0.0863) indicates that the isotherms are more likely to follow the Freundlich model than the Langmuir model [26]. This is also supported by the relatively low error computation results as shown in Table 5. Other investigations have found that Freundlich model fits better the experimental data on diclofenac adsorption than the Langmuir model, utilizing gelatin carbon nanotubes [26], multi-walled carbon nanotubes [29], activated carbon from *Persicum cyclamen* tubers [30], and grape bagasse [31], and commercial granular activated carbon [36].

Preprints (www.preprints.org) | NOT PEER-REVIEWED | Posted: 27 May 2022 doi:10.20944/preprints202205.0371.v1

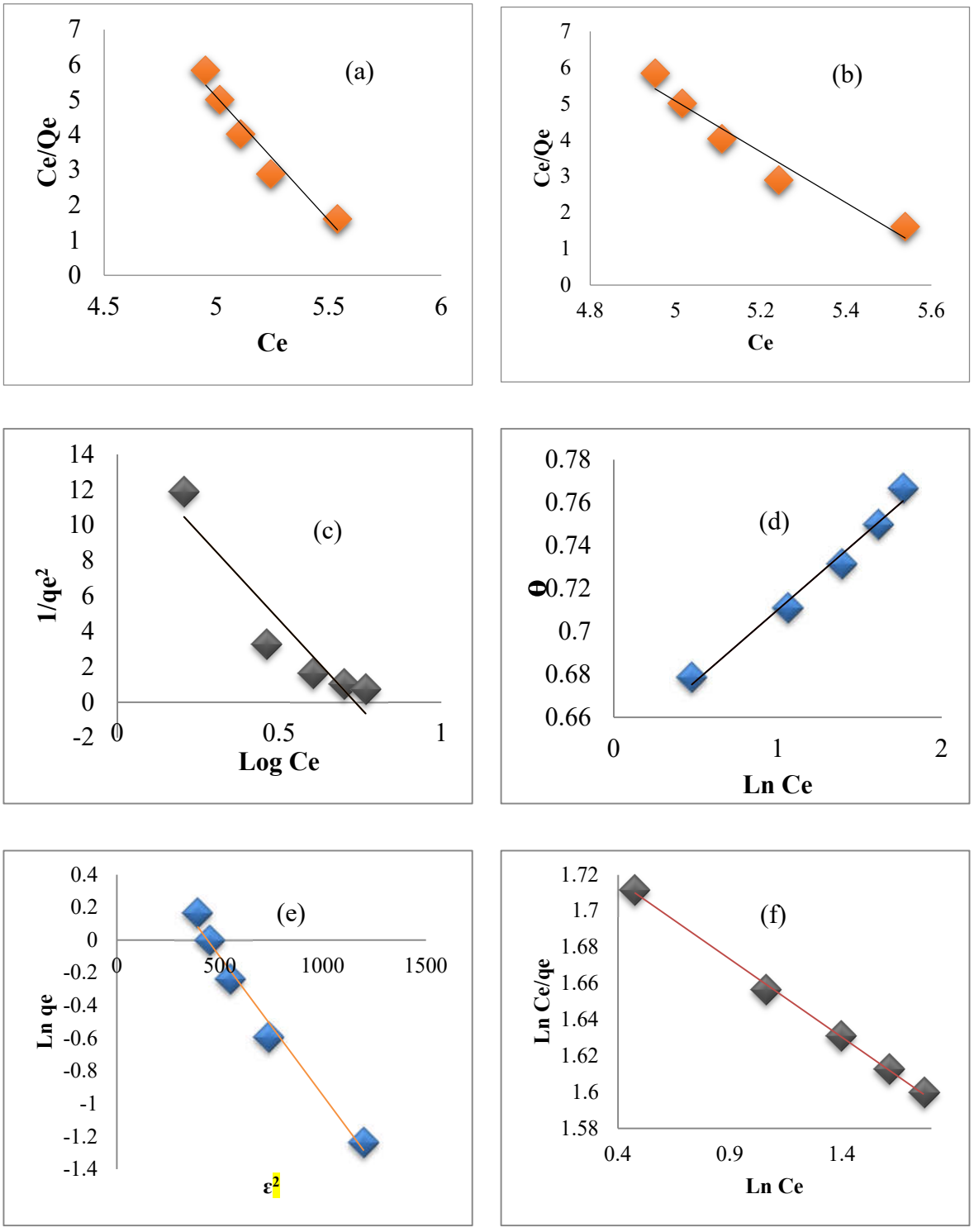

Figure 7. Adsorption isotherms of 10 mg/l DCF-Na onto 1 g of BKW composite. Fitting of the experimental data to (a) Langmuir (b) Freundlich (c) Harkin-Jura (d) Temkin (e)Dubinin-Radushkevich (f) Redlich-Peterson isotherm models carried out at room temperature (25 °C).

Preprints (www.preprints.org) | NOT PEER-REVIEWED | Posted: 27 May 2022 doi:10.20944/preprints202205.0371.v1

Table 5. Isotherm parameters for the adsorption of DCF-Na from modified clay composite.

Isotherm Models	Parameter	Values
Langmuir	Q_{max} (mg/g)	0.0025
	K_L (L/mg)	0.0047
	Multiple R	0.9566
	R Squared	0.9150
	Adjusted R Squared	0.8867
	Standard Error	5.65E-01
	SSE	0.96
	RMSE	1.20
Freundlich	K_F ((mg/g)(L/mg)$^{1/n}$)	0.1736
	n	1.086
	Multiple R	0.9999
	R Squared	0.9999
	Adjusted R Squared	0.9999
	Standard Error	0.0021
	SSE	0.000013
	RMSE	0.003752
Harkin-Jura	A	0.0504
	B	0.7340
	Multiple R	0.9450
	R Squared	0.8931
	Adjusted R Squared	0.8574
	Standard Error	1.77
	SSE	9.35
	RMSE	3.56
Temkin	B (L/g)	0.0663
	A (mol/KJ)$^{-1}$	164.88
	Multiple R	0.9918
	R Squared	0.9836
	Adjusted R Squared	0.9781
	Standard Error	0.01
	SSE	0.32
	RMSE	0.01
Dubinin-Radushkevich	Qm (mg/g)	2.1130
	R^2	0.9831
	Multiple R	0.9915
	R Squared	0.9831
	Adjusted R Squared	0.9775
	Standard Error	0.08
	SSE	0.32
	RMSE	0.69
Redlich-Peterson	B	-0.0863
	A	0.1736
	Multiple R	0.9992
	R Squared	0.9985
	Adjusted R Squared	0.9980
	Standard Error	0.001
	SSE	0.05
	RMSE	0.28

Preprints (www.preprints.org) | NOT PEER-REVIEWED | Posted: 27 May 2022 doi:10.20944/preprints202205.0371.v1

Table 6. Comparison of parameters of some adsorbents used for removal of DCF from aqueous solution.

Adsorbent	n	Q_{max} (mg/g)	K_L	K_F	References
Natural and pillared clay		62.50 – 100.00	0.056 – 0.053	0.039 – 0.0547	[33]
Activated Carbon prepared from olive stones	1.26	11.00	0.8090	0.4935	[34]
Activated Carbon	2.014 – 2.462	36.23 – 46.22	2.659 – 6.199	0.8865 – 2.712	[24]
Magnetic amine-functionalized chitosan	5.22	469.48	0.021	120.74	[35]
Modified BKW composite	1.086	0.0025	0.0047	0.1736	This study

Table 7. Comparison between the types of isotherms exhibited by different adsorbent–adsorbate relationship.

Adsorbent	Adsorbate	Q_{max} (mg/g)	R^2	Isotherms	References
Natural and pillared clay	Diclofenac Potassium	62.50 – 100.00	0.992 – 0.998	Langmuir	[33]
Activated Carbon prepared from olive stones	Diclofenac	11.00	0.9024	Braunuer-Emmett-Teller	[34]
Bentonite Clay	Cationic Dye	8.11	0.9970	Freundlich	[9]
Activated Carbon	Diclofenac	36.23 – 46.22	0.9680 – 0.9891	Freundlich	[24]
Magnetic amine-functionalized chitosan	Diclofenac	469.48	0.958	Langmuir	[35]
Modified BKW composite	Diclofenac	0.0025	0.999	Freundlich	This study

3.5. Adsorption Kinetics Models

Figure 8 shows the four kinetics models - Pseudo first order (PFO), Pseudo second order (PSO), Elovich, and Avrami employed in fitting the experimental data at 5, 10 and 15 mg/l DCF-Na concentrations. Table 8 shows the kinetics parameters and error analysis results of all the considered kinetics models. The PSO model (Figure 8a) gave a good fit of the experimental equilibrium adsorption data for all the considered concentrations, though the data appeared relatively less fitted at 15 mg/l which sort to invalidate Temkin's isotherm prediction of interactions between the adsorbent and the adsorbate without regard to low or high adsorbate concentrations. The error analysis results appeared to be relatively low when compared to PSO and Avrami model.

The variation between the qe_{cal} and qe_{exp} for all concentrations reveals that PSO does not appear to fit the adsorption data any better than pseudo-first order. The pseudo-second-order model's low R^2 values indicate its unsuitability in comparison to other models studied. This result is consistent with research that reported DCF-Na adsorption to fit the Freundlich isotherm model [37, 38]. This is also supported by the large error computation results as shown in Table 8.

The Elovich model (Figure 8c) demonstrates the applicability for kinetics far from equilibrium when desorption is not possible due to the adsorbent's limited surface coverage. The model parameters are presented in Table 8. In comparison to other kinetic models, the R^2 values were well matched, demonstrating the model's appropriateness. Elovich kinetics model gave the least Standard error, SSE and RMSE when compared to other kinetics models used in this study (Table 8).

The adsorption rate coefficient may have a temporal dependency throughout the adsorption process, according to the Avrami model (Figure 8d). The R^2 values indicate a good fit of the model in describing DCF-Na adsorption. The error analysis results appeared to be relatively low when compared and of comparable order of magnitude with the PFO.

Preprints (www.preprints.org) | NOT PEER-REVIEWED | Posted: 27 May 2022 doi:10.20944/preprints202205.0371.v1

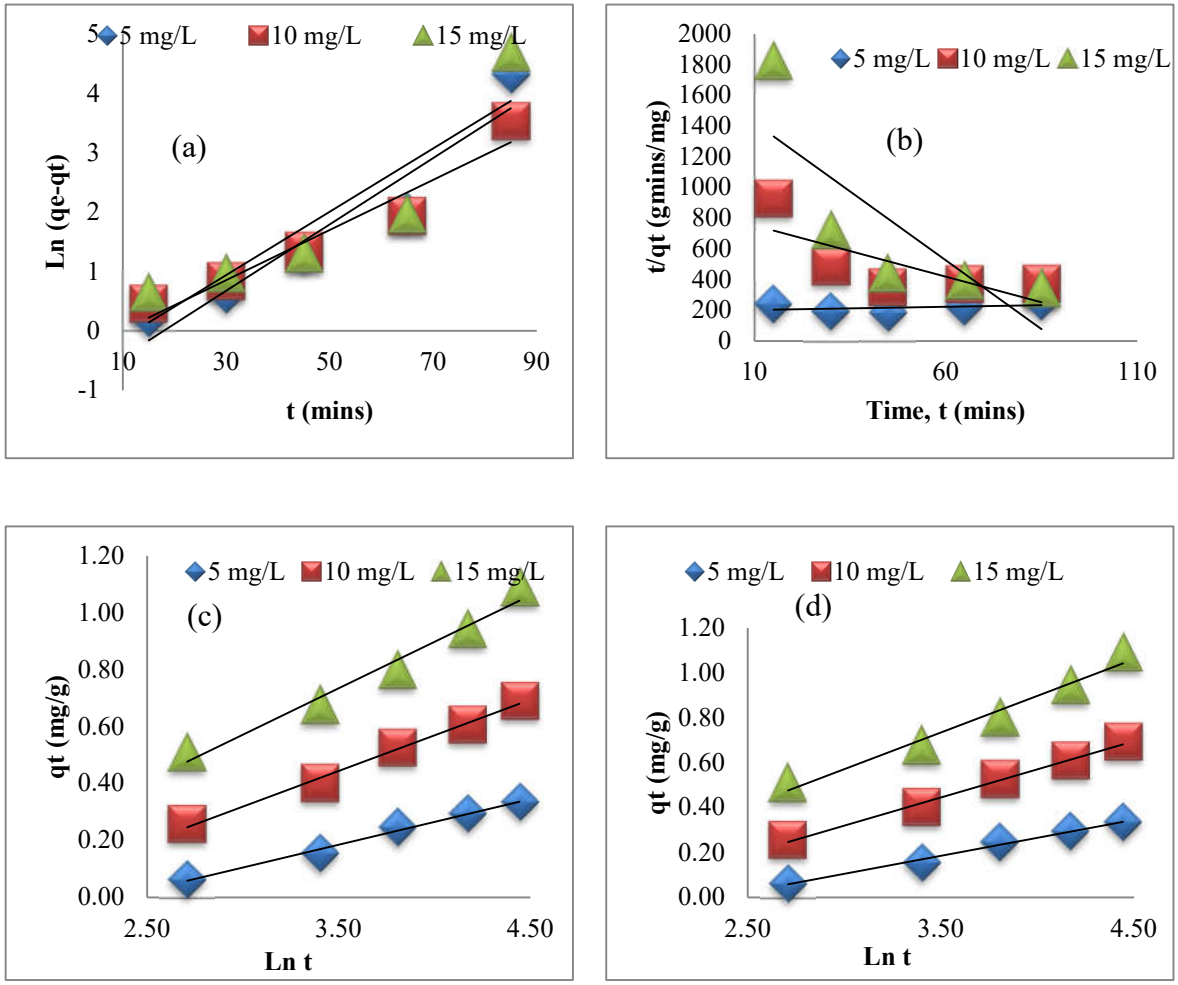

Figure 8. (a) Pseudo First Order Kinetics Model (b) Pseudo Second Order Kinetics Model (c) Elovich Model (d) Avrami Model for the removal of DCF-Na onto modified BKW composite.

Preprints (www.preprints.org) | NOT PEER-REVIEWED | Posted: 27 May 2022 doi:10.20944/preprints202205.0371.v1

Table 8. Kinetic model parameters for the adsorption of DCF-Na onto modified BKW composite.

Kinetics model	Kinetic model Parameters	Concentration (mg/l)		
		5	10	15
Pseudo 1st Order	K_1 (min^{-1})	-0.0558	-0.0422	-0.0533
	qe_{cal} (mgg^{-1})	0.3426	0.7190	1.1136
	qe_{exp} (mgg^{-1})	0.3512	0.7223	1.1065
	Multiple R	0.9559	0.9682	0.9118
	R Square	0.9138	0.9373	0.8315
	Adjusted R Square	0.8851	0.9165	0.7753
	Standard Error	0.5495	0.3496	0.7693
	SSE	0.91	0.385003	1.7757
	RMSE	1.07	0.707508	1.49
Pseudo 2nd Order	K_2 ($mg/g.min^{-1}$)	0.0932	0.0782	0.0766
	qe_{cal} (mgg^{-1})	2.3878	-0.1502.	-0.0533
	qe_{exp} (mgg^{-1})	-1.233	1.2567	0.0056
	Multiple R	0.3946	0.7537	0.7998
	R Square	0.1557	0.5681	0.6397
	Adjusted R Square	-0.1257	0.4241	0.5196
	Standard Error	31.2473	186.0263	431.2701
	SSE	2929.18	103817.31	557981.84
	RMSE	61.86	374.07	867.82
Elovich	A	0.6002	0.7087	0.8816
	B	0.1601	0.2506	0.3261
	Multiple R	0.9960	0.9975	0.7998
	R Square	0.9921	0.9949	0.6397
	Adjusted R Square	0.9895	0.9932	0.5196
	Standard Error	0.0112	0.0141	431.2701
	SSE	0.00038	0.00060	0.00526
	RMSE	0.01888	0.02796	0.08843
Avrami	N	1.6808	1.1472	1.0331
	K	39.3703	32.7909	28.3025
	Multiple R	0.8766	0.8894	0.8152
	R Square	0.7684	0.7911	0.6645
	Adjusted R Square	0.6912	0.7214	0.5526
	Standard Error	0.8671	0.6458	1.0171
	SSE	2.256	1.251	3.104
	RMSE	1.844	1.371	2.110
	Multiple R	0.8766	0.8894	0.8152

3.6. Adsorption Diffusion Mechanism

The effect of concentration on mass transfer diffusion was studied using four models: Crank diffusion models, Vermeulen model, Weber-Morris, and Banghams at DCF-Na concentration of 5, 10, 15 mg/l. Table 9 shows that the value of the models' regression coefficients is more than 0.8 for all which examines the goodness of fit. It is critical to consider the sorbent influence process rate in experimental data interpretation and learn about the DCF-Na mechanism adsorption on surfaces of BKW composite. Because active sorbent sites are within sorbent particles. The linearity of this curve at an early stage of the reaction, according to the Crank diffusion theory, indicates a diffusion-controlled sorption mechanism [19]. Figure 9a shows the Crank diffusion model plot. As can be observed, for modest values of time, a good linear relationship between the adsorbed DCF-Na and $t^{0.5}$ is achieved, indicating the importance of the diffusion mechanism in-Na remediation kinetics [36]. The plots from Vermeulen, Weber-Morris, and Banghams diffusion

Preprints (www.preprints.org) | NOT PEER-REVIEWED | Posted: 27 May 2022 doi:10.20944/preprints202205.0371.v1

models also provided a good fit in describing DCF-Na model. These models consider intra-particle diffusivity of DCF-Na onto the composite clay surface [20].

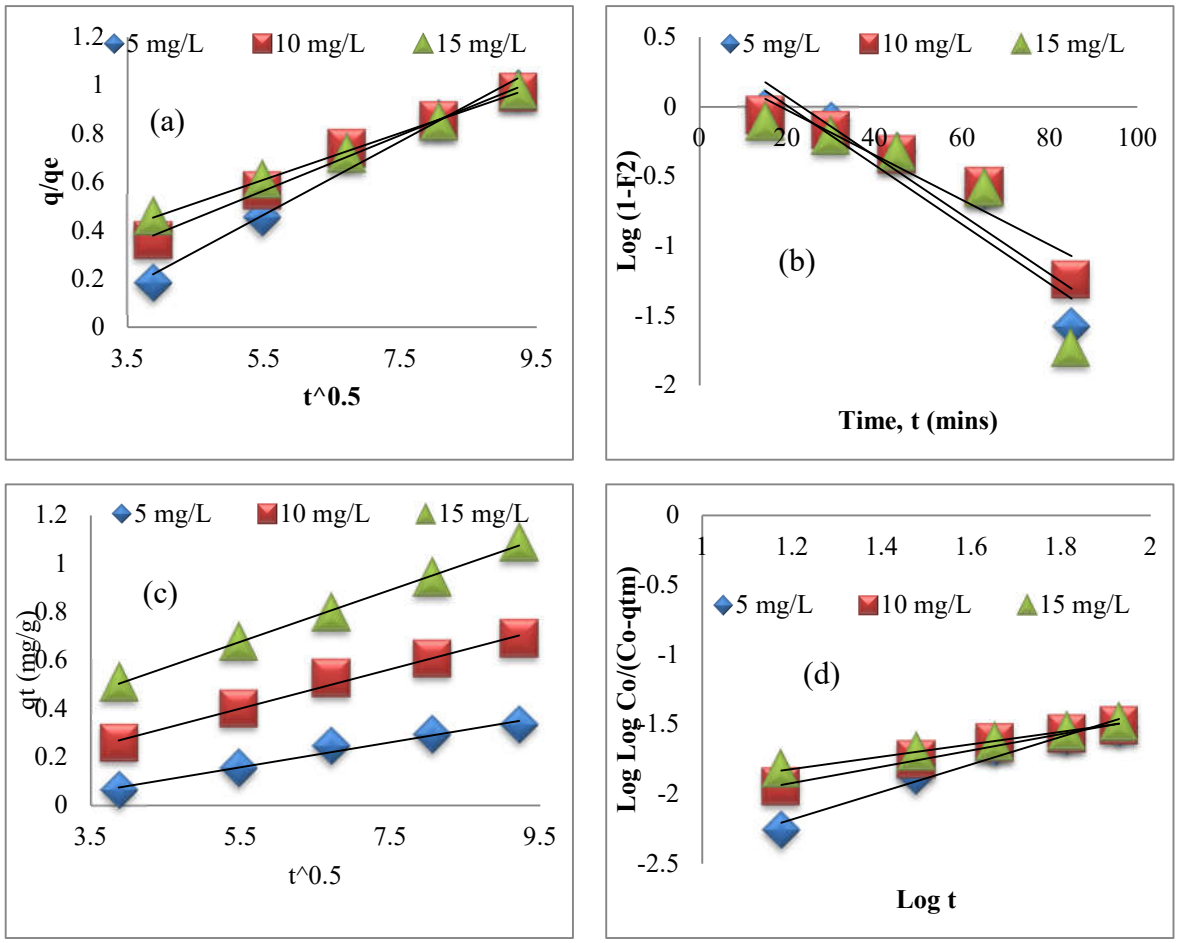

Figure 9.(a) Crank (b) Vermeulen (c) Weber Morris (d) Banghams diffusion model for the removal of DCF-Na from modified BKW composite.

Table 9. Mass transfer diffusion model calculated parameters for the adsorption of DCF-Na onto modified BKW composite.

Diffusion Model	Parameters	Concentration		
		5 mg/l	10 mg/l	15 mg/l
Crank (Boyd)	R^2	0.9789	0.9915	0.9984
	R (μm)	36.1533	20.5243	14.6296
Vermeulen (Dumwald Wagner)	R^2	0.8679	0.9063	0.8012
	K ($L.min^{-1}$)	0.0488	0.0371	0.0491
Weber-Morris	R^2	0.8679	0.9063	0.8012
	K ($mg/g.min^{-0.5}$)	-0.0212	-0.0161	-0.0213
Banghams	R^2	0.9614	0.9912	0.9975
	θ	0.9879	0.5871	0.4447

3.7. Thermodynamics Study

Adsorption process is measured by the thermodynamics parameters such as Gibb's free energy change (ΔG°), Entropy change (ΔS°) and the Enthalpy change (ΔH°) as a result of the solute transfer onto liquid-solid interface [15]. As illustrated in Figure 10, the parameters were analyzed using Vant Hoff's plot. The DCF-Na molecule's partitioning coefficient Kd (l/mol) towards the adsorbent is also an important metric to consider while studying DCF-Na molecule movement through BKW composite adsorbent. The values of

Preprints (www.preprints.org) | NOT PEER-REVIEWED | Posted: 27 May 2022 doi:10.20944/preprints202205.0371.v1

ΔG° are negative for all the temperatures (Table 10). The decrease in the value of Gibb's free energy change (ΔG°) as temperature increases showed that the adsorption process decreases with rising temperature. Also, the change in the free energy change might be due to the rise in the degree of freedom which could augment the desorption rate rather than adsorption rate at an increasing temperature [29]. The values of Gibb's free energy estimated were within the range (-20 – 0 kJ/mol) of the physisorption process [37] and the enthalpy change (ΔH°) values varied from -4.1293 kJ/mol to -12.2723 kJ/mol indicating an exothermic adsorption mechanism and confirming the spontaneity of DCF-Na adsorption onto modified BKW [38]. Also, the negative values of ΔS° confirm the randomness decrease between the solute/solid interface [37]. The parameters values of the Gibb's free energy, Enthalpy change, and Entropy change are compared with other studies that used different adsorbents for the remediation of DCF-Na from wastewater (Table 11).

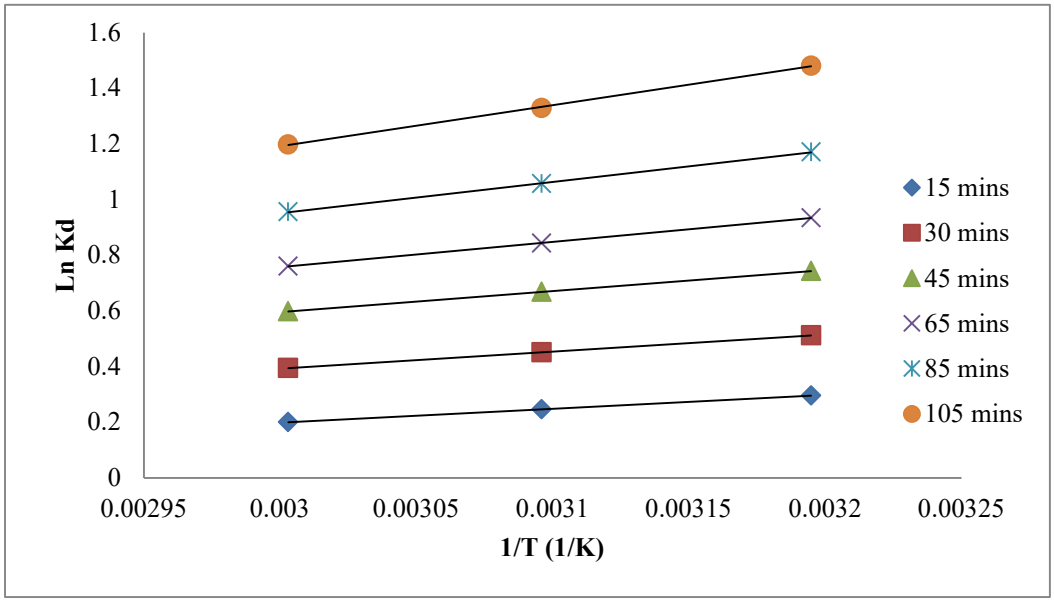

Figure 10. Vant Hoff's model plot for DCF-Na removal from solution onto modified BKW composite.

Preprints (www.preprints.org) | NOT PEER-REVIEWED | Posted: 27 May 2022 doi:10.20944/preprints202205.0371.v1

Table 10. Thermodynamic parameters for DCF-Na removal from solution onto modified BKW composite.

Time (mins)	Temperature (K)	K_d	Ln K_d	ΔG (kJ/mol)	ΔH (kJ/mol)	ΔS (kJ/mol K)
	313	1.3444	0.2960	-0.7705		
15	323	1.2804	0.2472	-0.6632	-4.1293	-0.0107
	333	1.2222	0.2007	-0.5559		
	313	1.6690	0.5122	-1.3328		
30	323	1.5714	0.4520	-1.2134	-5.0700	-0.0119
	333	1.4847	0.3952	-1.0940		
	313	2.1043	0.7440	-0.4228		
45	323	1.9516	0.6687	-0.2833	-4.7879	-0.1395
	333	1.8195	0.5986	-0.1439		
	313	2.5474	0.9351	-2.4324		
65	323	2.3269	0.8445	-2.2699	-7.5188	-0.0163
	333	2.1416	0.7615	-2.1074		
	313	3.2267	1.1714	-3.0463		
85	323	2.8810	1.0581	-2.8458	-9.3225	-0.0201
	333	2.6022	0.9563	-2.6453		
	313	3.4571	1.2404	-3.5807		
105	323	3.0633	1.1195	-3.5817	-12.2723	-0.0269
	333	2.7500	1.0116	-3.3126		

Table 11. Comparison of modified BKW composite and some adsorbents in relation to DCF-Na remediation.

Adsorbent	ΔG°	ΔH°	ΔS°	Reference
Natural and Pillared Clay	-0.0194	10.20	0.093	[33]
Ionosilicas	-1.8665	-32.70	-0.1265	[39]
Coupled Organo clay	-13.695	-212.40	-0.6488	[25]
Carbon nanotubes polytetrafluoroethylene	-4.2654	-8.8212	-0.0148	[40]
BKW composite	-3.3126	-12.27	-0.0269	This study

4. Conclusion

The clay samples' ion exchangeability was improved by modifying their surfaces. For the removal of DCF-Na from aqueous solutions into the BKW composite, the effect of concentration and dose on adsorption was investigated. The adsorption capacity and removal efficiency improve with increasing concentration of DCF-Na. Compared to other isotherm models, the Freundlich isotherm model provided a better fit. In contrast to other kinetics models, the Elovich kinetic model provided a better understanding of the kinetics of DCF-Na adsorption onto changed surfaces. The adsorption is exothermic, viable, and heterogeneous. In conclusion, the BKW composite performed exceptionally well in removing DCF-Na from wastewater.

Acknowledgments: The Bioenvironmental Water and Engineering Research Group, Department of Chemical Engineering, Ladoke Akintola University of Technology, Ogbomoso, Oyo State, Nigeria, is grateful for their assistance.

Conflicts of Interest: The authors declare no conflict of interest.

References

1 Hombal P, Gudadappanavar A, Kavi A (2016) International Surgery Journal 557–561. http://dx.doi.org/10.18203/2349-2902.isj20160702
2 Zhang Y, Geißen S-U, Gal C (2008) Chemosphere 73:1151–1161. http://dx.doi.org/10.1016/j.chemosphere.2008.07.086
3 Acuña V, Ginebreda A, Mor JR, Petrovic M, Sabater S, Sumpter J, et al. (2015) Environment International 85:327–333. http://dx.doi.org/10.1016/j.envint.2015.09.023
4 Lonappan L, Brar SK, Das RK, Verma M, Surampalli RY (2016) Environment International 96:127–138. http://dx.doi.org/10.1016/j.envint.2016.09.014
5 Memmert U, Peither A, Burri R, Weber K, Schmidt T, Sumpter JP, et al. (2013) Environmental Toxicology and Chemistry 32:442–452. http://dx.doi.org/10.1002/etc.2085
6 Sadanand P, James R (2016) American Journal of Chemistry and Applications 3:8–19.
7 Figueroa RA, Leonard A, MacKay AA (2004) Environmental Science & Technology 38:476–483. http://dx.doi.org/10.1021/es0342087
8 Crini G, Lichtfouse E (2019) Environmental Chemistry Letters 17:145–155. http://dx.doi.org/10.1007/s10311-018-0785-9
9 Obiageli R (2017) ADSROPTION OF CATIONIC DYE ONTO LOW-COST ADSORBENT SYNTHESIZED FROM BENTONITE CLAY Part I . KINETIC AND THERMODYNAMIC STUDIES Ajemba
10 Bhadra BN, Seo PW, Jhung SH (2016) Chemical Engineering Journal 301:27–34. http://dx.doi.org/10.1016/j.cej.2016.04.143
11 Yoon S-Y, Lee C-G, Park J-A, Kim J-H, Kim S-B, Lee S-H, et al. (2014) Chemical Engineering Journal 236:341–347. http://dx.doi.org/10.1016/j.cej.2013.09.053
12 Osagie EI, Owabor CN (2015) Advances in Chemical Engineering and Science 05:345–351. http://dx.doi.org/10.4236/aces.2015.53036
13 Wu C, Xiong Z, Li C, Zhang J (2015) RSC Advances 5:82127–82137. http://dx.doi.org/10.1039/C5RA15497A
14 Okeowo IO, Balogun EO, Ademola AJ, Alade AO, Afolabi TJ, Dada EO, et al. (2020) International Journal of Environmental Research 14:215–233. http://dx.doi.org/10.1007/s41742-020-00244-7
15 Ayawei N, Ebelegi AN, Wankasi D (2017) Journal of Chemistry 2017:1–11. http://dx.doi.org/10.1155/2017/3039817
16 Redlich O, Peterson DL (1959) The Journal of Physical Chemistry 63:1024–1024. http://dx.doi.org/10.1021/j150576a611
17 Cestari AR, Vieira EFS, dos Santos AGP, Mota JA, de Almeida VP (2004) Journal of Colloid and Interface Science 280:380–386. http://dx.doi.org/10.1016/j.jcis.2004.08.007
18 Coulson CA (1958) The Mathematical Gazette 42:165–165. http://dx.doi.org/10.2307/3609455
19 Vermeulen T (1953) Industrial & Engineering Chemistry 45:1664–1670. http://dx.doi.org/10.1021/ie50524a025
20 Hoskins WM, Bray WC (1926) Journal of the American Chemical Society 48:1454–1474. http://dx.doi.org/10.1021/ja01417a002
21 Aharoni C, Sideman S, Hoffer E (2007) Journal of Chemical Technology and Biotechnology 29:404–412. http://dx.doi.org/10.1002/jctb.503290703
22 Jodeh S, Abdelwahab F, Jaradat N, Warad I, Jodeh W (2016) Journal of the Association of Arab Universities for Basic and Applied Sciences 20:32–38. http://dx.doi.org/10.1016/j.jaubas.2014.11.002
23 Mabrouki H, Akretche DE (2016) Desalination and Water Treatment 57:6033–6043. http://dx.doi.org/10.1080/19443994.2014.1002008
24 Larous S, Meniai A-H (2016) International Journal of Hydrogen Energy 41:10380–10390. http://dx.doi.org/10.1016/j.ijhydene.2016.01.096
25 Liang XX, Omer AM, Hu Z, Wang Y, Yu D, Ouyang X (2019) Chemosphere 217:270–278. http://dx.doi.org/10.1016/j.chemosphere.2018.11.023
26 Chang F, Memon N, Memon S, Chang AS (2022) International Journal of Environmental Science and Technology. http://dx.doi.org/10.1007/s13762-021-03882-2
27 de Franco MAE, de Carvalho CB, Bonetto MM, Soares R de P, Féris LA (2017) Journal of Cleaner Production 161:947–956. http://dx.doi.org/10.1016/j.jclepro.2017.05.197
28 de Oliveira T, Guégan R (2016) Environmental Science & Technology 50:10209–10215. http://dx.doi.org/10.1021/acs.est.6b03393
29 Rigueto CVT, Rosseto M, Nazari MT, Ostwald BEP, Alessandretti I, Manera C, et al. (2021) Journal of Environmental Chemical Engineering 9:105030. http://dx.doi.org/10.1016/j.jece.2021.105030
30 Liu J, Wang X (2013) The Scientific World Journal 2013:1–6. http://dx.doi.org/10.1155/2013/897159
31 Maia GS, de Andrade JR, da Silva MGC, Vieira MGA (2019) Powder Technology 345:140–150. http://dx.doi.org/10.1016/j.powtec.2018.12.097
32 Czech B, Kończak M, Rakowska M, Oleszczuk P (2021) Journal of Cleaner Production 288:125686. http://dx.doi.org/10.1016/j.jclepro.2020.125686
33 Zhao H, Liu X, Cao Z, Zhan Y, Shi X, Yang Y, et al. (2016) Journal of Hazardous Materials 310:235–245. http://dx.doi.org/10.1016/j.jhazmat.2016.02.045
34 Jodeh S, Abdelwahab F, Jaradat N, Warad I, Jodeh W (2016) Journal of the Association of Arab Universities for Basic and Applied Sciences 20:32–38. http://dx.doi.org/10.1016/j.jaubas.2014.11.002
35 Antunes M, Esteves VI, Guégan R, Crespo JS, Fernandes AN, Giovanela M (2012) Chemical Engineering Journal 192:114–121. http://dx.doi.org/10.1016/j.cej.2012.03.062

36 Huang L, Mao N, Yan Q, Zhang D, Shuai Q (2020) ACS Applied Nano Materials 3:319–326. http://dx.doi.org/10.1021/acsanm.9b01969
37 Lu X, Shao Y, Gao N, Chen J, Zhang Y, Wang Q, et al. (2016) Chemosphere 161:400–411. http://dx.doi.org/10.1016/j.chemosphere.2016.07.025
38 Moral-Rodríguez AI, Leyva-Ramos R, Ania CO, Ocampo-Pérez R, Isaacs-Páez ED, Carrales-Alvarado DH, et al. (2019) Environmental Science and Pollution Research 26:6141–6152. http://dx.doi.org/10.1007/s11356-018-3991-x
39 Salvestrini S, Fenti A, Chianese S, Iovino P, Musmarra D (2020) Journal of Environmental Chemical Engineering 8:104105. http://dx.doi.org/10.1016/j.jece.2020.104105
40 Rani S, Sud D (2016) Plant, Soil and Environment 61:36–42. http://dx.doi.org/10.17221/704/2014-PSE